EUROPEAN SYNCHROTRON RADIATION FACILITY

INSTALLATION EUROPEENNE DE RAYONNEMENT SYNCHROTRON

Experiment Report Form

ESRF

The double page inside this form is to be filled in by all users or groups of users who have had access to beam time for measurements at the ESRF.

Once completed, the report should be submitted electronically to the User Office via the User Portal: *https://wwws.esrf.fr/misapps/SMISWebClient/protected/welcome.do*

Deadlines for submission of Experimental Reports

Experimental reports must be submitted within the <u>period of 3 months</u> after the end of the experiment.

Experiment Report supporting a new proposal ("relevant report")

If you are submitting a proposal for a new project, or to continue a project for which you have previously been allocated beam time, <u>you must submit a report on each of your previous measurement(s)</u>:

- even on those carried out close to the proposal submission deadline (it can be a *"preliminary report"),*
- even for experiments whose scientific area is different form the scientific area of the new proposal,
- carried out on CRG beamlines.

You must then register the report(s) as "relevant report(s)" in the new application form for beam time.

Deadlines for submitting a report supporting a new proposal

- ➤ 1st March Proposal Round - **5th March**
- ➤ 10th September Proposal Round - **13th September**

The Review Committees reserve the right to reject new proposals from groups who have not reported on the use of beam time allocated previously.

Reports on experiments relating to long term projects

Proposers awarded beam time for a long term project are required to submit an interim report at the end of each year, irrespective of the number of shifts of beam time they have used.

Published papers

All users must give proper credit to ESRF staff members and proper mention to ESRF facilities which were essential for the results described in any ensuing publication. Further, they are obliged to send to the Joint ESRF/ ILL library the complete reference and the abstract of all papers appearing in print, and resulting from the use of the ESRF.

Should you wish to make more general comments on the experiment, please note them on the User Evaluation Form, and send both the Report and the Evaluation Form to the User Office.

Instructions for preparing your Report

- fill in a separate form for <u>each project</u> or series of measurements.
- type your report in English.
- include the experiment number to which the report refers.
- make sure that the text, tables and figures fit into the space available.
- if your work is published or is in press, you may prefer to paste in the abstract, and add full reference details. If the abstract is in a language other than English, please include an English translation.

![ESRF logo]	**Experiment title:** Tracking the evolution of transition metal single atom catalysts for the CO2 electroreduction: an operando HERFD XANES and XES study	**Experiment number**: CH6522
Beamline:	**Date of experiment**: from: 4/10/2022 to: 12/10/2022	**Date of report**: 12/02/2023
Shifts:	**Local contact(s)**: Viktoria Saveleva	*Received at ESRF:*
Names and affiliations of applicants: Andrea Martini, Janis Timoshenko, Philipp Grosse and Clara Rettenmaier.		

Report:

With the following report, we are showing the results of the analysis of the Ni Transition metal-nitrogen-doped carbons (TMNC) system [1] using XAS and XES methods. The synchrotron based measurements were performed in *operando* conditions with the main purpose to track and differentiatiate among the different Ni-reaction intermediates and products appearing and evolving during the CO_2 electrochemical reduction reaction (CO_2RR).

For our experiments we used our single compartment electrochemical cell (see **Figure 1**) suitable for X-ray spectroscopy experiments. The cell was oriented of 45° with respect to the incident beam, in order to maximise the detected fluorescence signal deriving from the sample and suppress the elastic scattering [2]. The cell features a typical three electrode setup, represented by a reference (Ag/AgCl electrode), a counter (Pt mesh) and a working electrode. The latter consists of a carbon paper supports (Freudenberg H15C13, Fuel Cell Store) on which the sample was deposited as an ink through a spray-coating technique (ca. 1.6 ± 0.1 mg of catalysts per cm^2).
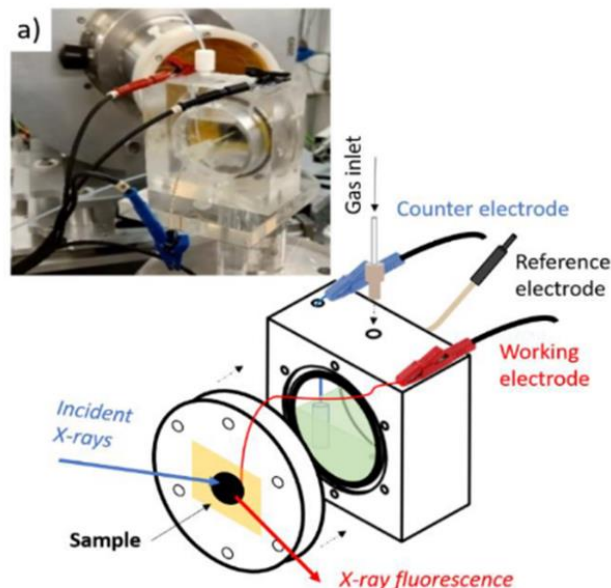
Figure 1: Schematics of the electrochemical setup used for our measurements [2].

The measurements were performed in a CO_2-saturated 0.1 M $KHCO_3$ electrolyte under a static current of -10 mA, corresponding to a current density of -15.7 mA/cm^2. The applied current was controlled by a *BioLogic* potentiostat.

Ni K-edge high energy resolution fluorescence detected (HERFD) X-ray absorption near edgestructure (XANES) and valence to core (vtc) $K\beta_{2,5}$ X-ray emission spectroscopy (XES) measurements were performed at the ESRF beamline ID26. The storage ring operated in 7/8 multibunch mode with an electron current of 200 mA. Three undulators produced the incoming radiation, which was monochromatized by a pair of Si (111) crystals, cryogenically cooled. The energy calibration of the incident beam was done using a reference metallic Ni foil by setting the first reflection point of the Ni K edge to 8333 eV. HERFD XANES spectra were collected in a continuous scan mode by varying the incident energy from 8320 to 8450 over Ni K edge with an energy step 0.1 eV and duration 40 seconds per spectrum. The maximum of the Ni $K\beta$ fluorescence line (8266.8 eV) was selected with an emission spectrometer in Rowland geometry with five Ge (620) analyzer crystals (R = 1 m) aligned at Bragg angel of 79.09°. The emission spectrometer was aligned using the elastic peak at $K\beta$ fluorescence energy. Si avalanche photodiode (APD) with 200 μm thickness and 10 x 10 mm^2 active area was used as a detector. The position of the beam on the sample was changed after each scan to minimize the possible beam damage, where in total 12 spots have been probed in case of HERFD XANES and vtc-XES. Spectra were normalized by the incoming flux recorded by detecting the scattering from a Kapton foil with a photo diode.

As a first step of our investigation, we tried to follow the CO_2RR reaction for one hour using HERFD XANES. The collected spectra were normalised for the absorption jump using the ATHENA software and are shown in **Figure 2**.
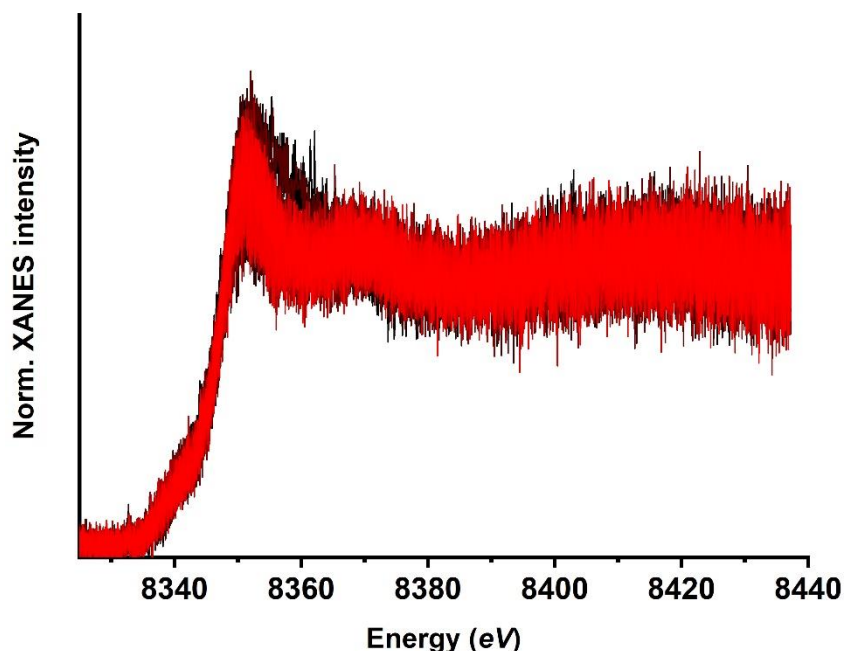
Figure 2: Ninety Ni K-edge HERRFD-XANES spectra acquired during CO$_2$RR. The color of the signals follow the acquisition order and it goes from black to red.

As it is possible to see, the spectra are affected by a low signal to noise ratio (in the flat region of the pre-edge between 8318 and 8330 eV the mean value of normalized spectrum is ca 0.006 with a standard deviation of 0.03) which can be attributed, mainly, to the low loading of Ni sites in the carbon matrix [3].

Nonetheless, we saw that the spectra quality was sufficient to enable the spectra interpretation using the principal component analysis (PCA) [4].

The PCA analysis of the HERFD-XANES dataset of **Figure 2** is shown in **Figure 3**.
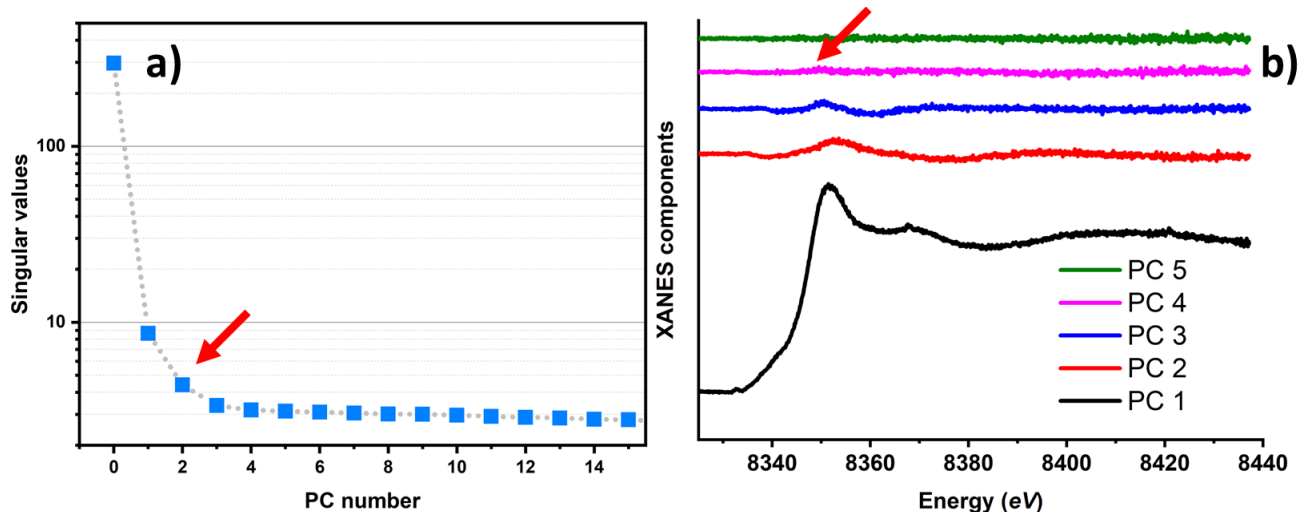

Figure 3: (a) Scree plot: singular values - variances associated to each principal component plotted *vs* the component number. (b) Abstract spectra: principal components extracted by PCA. The red arrows indicate the correct number of pure components in the catalyst, as obtained by PCA.

Despite the fact that the Scree plot (i.e., singular values extracted by PCA plotted *vs* the number of components) shows in **Figure 3**(a) an elbow in proximity of the third component, the analysis of each single compomponent, provided by the PCA, indicates that the fourth principal component also exhibit spectroscopically meaningful features (see **Figure 3**(b)), while the fifth and furthere principal components encodes just experimental noise. In accordance with this evidence, we supposed the existence of four chemical species evolving during CO$_2$RR conditions. Herein it is worth underlying that in our previous analysis performed on a similar catalysts (collected in conventional XAS mode at Bessy II -KMC 3 beamline)

we found that the dataset could be represented by just three components (Martini et al., in preparation). We assumed then that the presence of an additional species could be associated to a radiation damage effect.

The extraction of the HERFD XANES spectra corresponding to each species was realised using the transformation matrix approach [5] as implemented in the PyFitIt code [6]. The MCR-ALS technique [7], that nowadyas is becoming very popular in the XAFS community, was also tried out, but was unable to reach a convergent solution using the dataset shown in **Figure 2**.

The XANES spectra, isolated by transformation matrix approach, and corresponding concentrations profiles are reported in **Figure 4**.
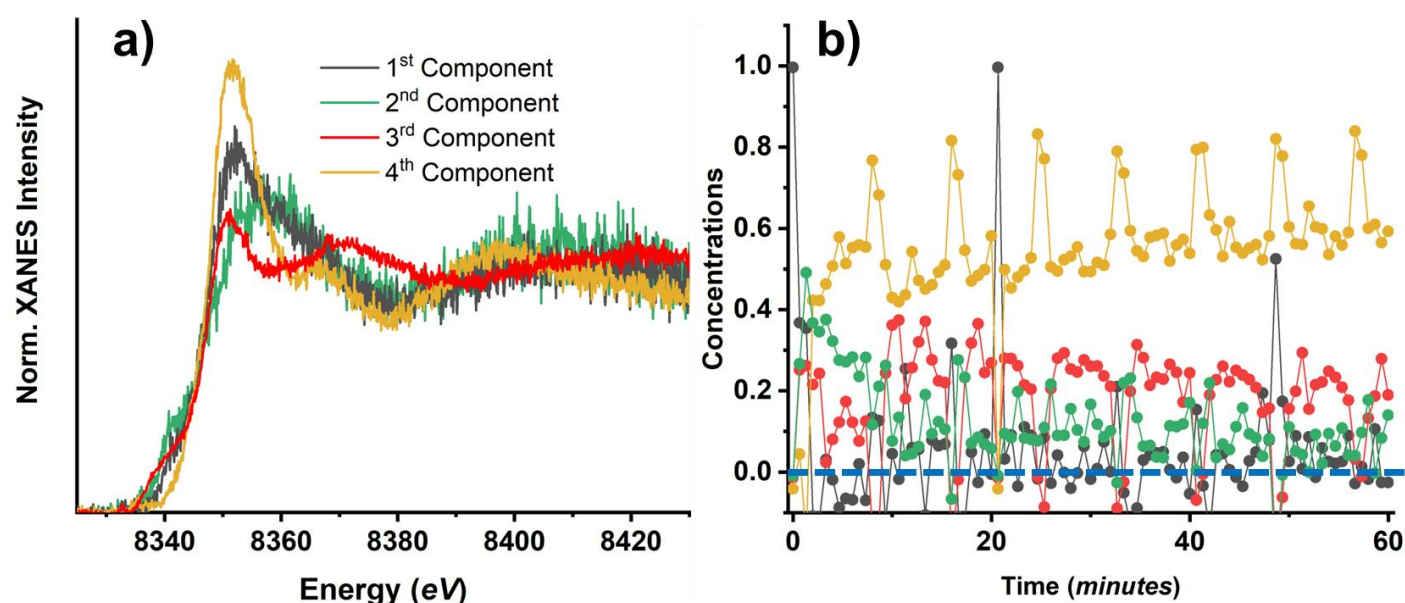

Figure 4: Set of XANES spectra (a) and related concentration profiles extracted through the transformation matrix approach as implemented in the PyFitIt code. The periodic behaviour that can be clearly noted looking at the concentration profiles is linked to the periodic movement of the sample during the measurments. The beam was continuosly moved to twelve different points in the sample. Once it reached the twelth-one it returned back to the initial (first) position. The blue line in b) indicates the zero concentration. Due to the large intrinsic noise in the data, some concentration values are slighty lower than this value.

The first component, identified by PCA and by the transformation matrix approach, can be associated with a six coordinated model where the Ni site is bound to four N atoms belonging, in turn, to a molecular ring composed by four pyridines in planar geometry, and to two axial O atoms. As the reaction proceeds the pyridines ring is further distorted and, progressively, the two O atoms are substituted by two CO ligands, giving rise to the second (five coordinated intermediate of reaction with one CO group) and third component (final state with a distorted octahedral geometry possessing two CO groups). The formation of the catalyst's final state is relatively fast and required just ten minutes. Afterwards the contribution of the Ni species bound to the two CO groups is stabilised to a contant concentration value of ca. 30%.

The fourth component identified by the transformation matrix approach, coincides with the reference spectrum for $Ni(OH)_2$ (β-form) spectrum and, as indicated before, we associate its presence to a beam effect. The formation of $Ni(OH)_2$ had the largest impact on the concentration of Ni species bound to the two CO groups.

In order to obtain more insights on the catalysts speciation and in particular to validate the suggested structures, we acquired the Ni vtc-$K\beta_{2,5}$ XES spectra of the sample in the initial state (in air before the reaction) and during CO_2RR, respectively. The collected spectra are reported in **Figure 5**. The background of the all XES signals was removed using Voight functions with common interpolation ranges. Afterwards the background subtracted curves were normalised by

their variance using the formula: $\frac{1}{(E_{max} - E_{min})} \int_{E_{min}}^{E_{max}} XES^2(E) dE$, where the E_{max} and E_{min} are the extreme values
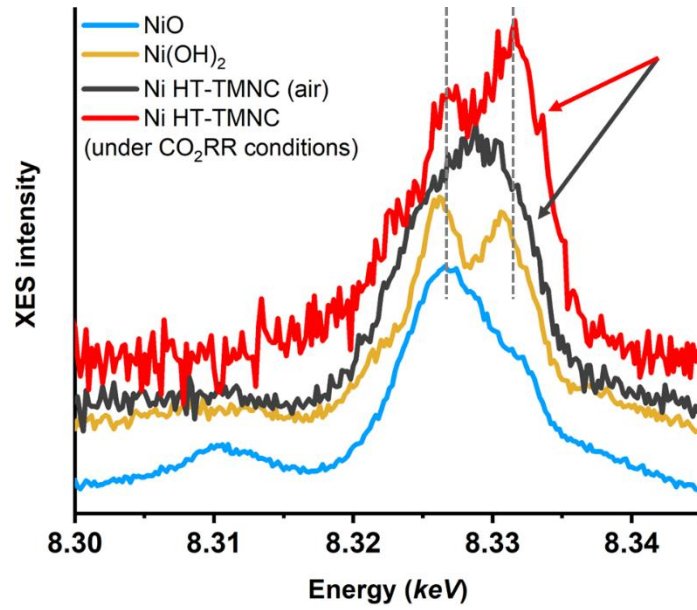
of the selected energy range.

Figure 5: Ni vtc-$K_{\beta2,5}$ XES spectra acquired for the catalysts initial state (in air before the reaction), during CO_2RR and for two reference materials represented by the Ni(OH)$_2$ and NiO. The grey dashed lines are indicating that the two vtc-XES peaks of the catalysts during CO_2RR are not matching the ones of the Ni(OH)$_2$.

While from **Figure 4**(b) we expect a significant amount of Ni(OH)$_2$ contributing to the sample-averaged data, , it is evident

that the vtc-XES spectra, shown in **Figure 5**, collected for the initial state and during CO_2RR, differ noticeably from the

spectrum of Ni(OH)$_2$. In particular the vtc-XES spectrum of the initial state shows two shoulders (the one at ca. 8.33 keV

slighty more intense) corresponding to the main peaks of the Ni(OH)$_2$ but also an additional feature peak where the

Ni(OH)$_2$ vtc-XES spectrum has a minimum point. Furthermore, the positions of two main peaks of vtc-XES spectrum

collected during CO_2RR do not match with the energies of the main features of Ni(OH)$_2$. In addition, their intensity ratio

is inverted compared to the latter. Overall, all these qualitative evidences indicate that the two states, in air and during

CO_2RR, can be linked to the two Ni complexes with different ligands and distortions, coexisitng with a Ni(OH)$_2$ phase.

We tried to confirm these finding by simulating the Ni vtc-$K_{\beta2,5}$ XES spectra for these two states. To do so, following

approach was used. First, we fitted the HERFD XANES spectra of the first and third component using the Machine

Learning indirect approach [6, 8] and the FDMNES code for the construction of training datasets [9]) . The results of these

fits are shown in **Figure 6** and agree well with the results found in our previous work (Martini et al., in preparation).

Table 1: Best fit result obtained fitting the HERFD XANES spectra for the first and third components showed in **Figure 4** and in **Figure 6**.

Refined parameters	Best fit values
First Component fit	
Ni -Odistances	2.00 Å
Ni-N distances to the two pyridines N atoms closer to the Ni site	1.78 Å
Ni-N distances to the two pyridines N atoms farer from the Ni site	2.08 Å
Third Component fit	
Ni-CO distances	1.75 Å
Ni-N distances to the two pyridines N atoms closer to the Ni site	1.85 Å
Ni-N distances to the two pyridines N atoms farer from the Ni site	2.22 Å

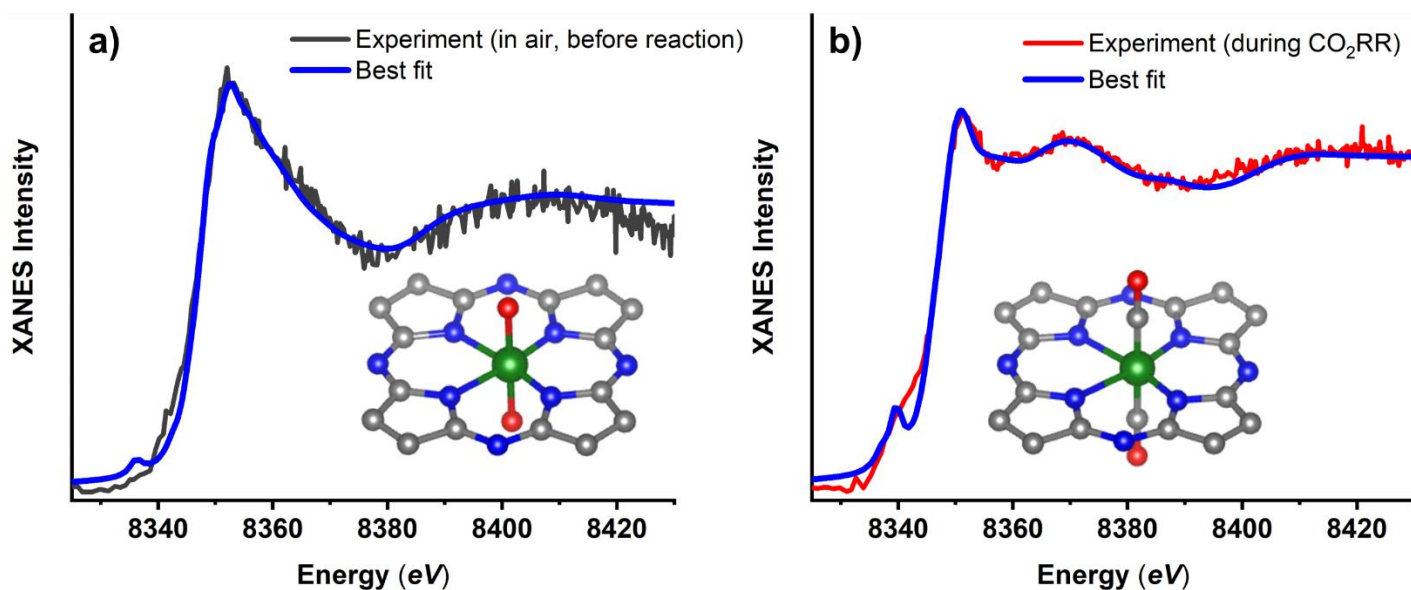| C-O distance within the CO group	1.28 Å
Ni-C-O angle	179 °

Figure 6: Experimental spectra (components) extracted from the dataset shown **Figure 1**, compared with the theoretical best fit spectra obtained through the PyFitIt approach. The insets show the refined geometries. Color code: Green: Ni, Oxygen: Red, Blue: N, Grey: C.

Afterwards we used these optimized structures to generated the corresponding vtc-XES spectra. FDM approach, as implemented in FDMNES code, was used for this purpse. Herein we broadened the unconvoluted XES spectra peaks with Gaussians functions having a FWHM value of 1.6 eV, corresponding to the energy resolution of the data acquisition evaluated taking the FWHM of the $K\beta_{1,3}$ emission line. The intensities and the energy shift of the theoretical spectra were optimized by minimizing the quantity $\|XES(E) - C \cdot XES(E + \Delta E)_{TEO}\|^2$, where C and ΔE are the required constants needed to achive the highest similarity with the experiment, respectively.

We tested this approach before on a known compound, the Ni-Phthalocyanine (see **Figure 7**), that allowed us to confirm the realiability of the results obtained using the FDMNES code.
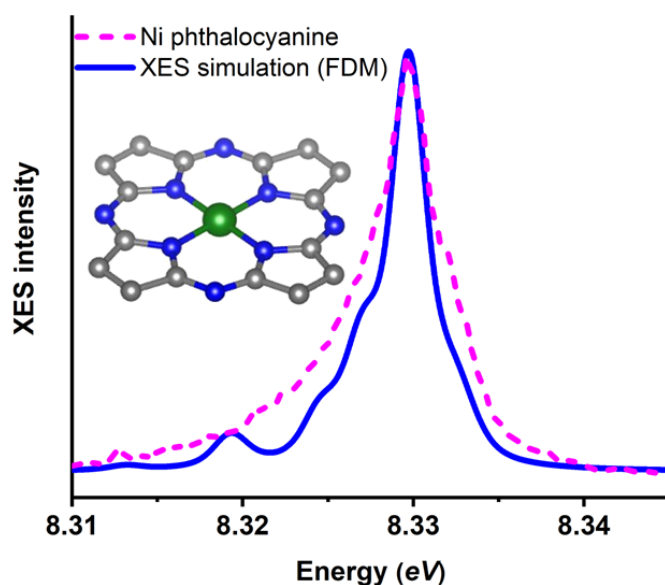

Figure 7: Comparison between the experimental and theoretical Ni vtc-$K\beta_{2,5}$ spectra for the reference Ni-Phthalocyanine compound. Color code: Green: Ni, Blue: N, Grey: C.

The vtc-XES spectra calculated for Ni TMNC catalysts are reported in **Figure 8**. We note that both for the initial state of the catalyst and for the final state, the calcualted vtc-XES spectra are similar due to the similar octahedral enviroment of

the Ni sites in these two cases. The relative shift between the two spectra were obtained by shifting the two signals by their corresponding EPSII values plus an additional quantity obtained by centering the theoretical Ni-Phthalocyanine theretical spectrum with respect to the experiment.
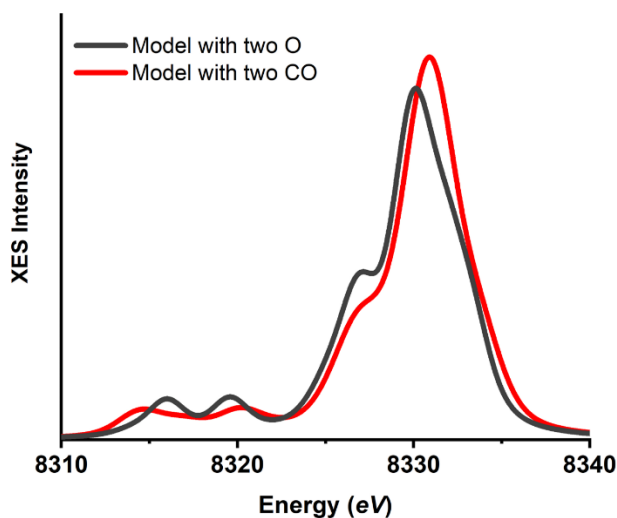

Figure 8: Calculated Ni vtc-K$\beta_{2,5}$ spectra for Ni-TMNC catalyst in air and under CO$_2$RR. The two spectra have been simulated starting from the refined structures shown in **Figure 6**.

Since the experimental XES spectra shown in **Figure 5** are expected to contain significant Ni(OH)$_2$ contributions, we decided to estimate the fractions of the two Ni single sites reported in the insets of **Figure 6**. These quantities were obtained by minimising the following quantity: $\|XES_{exp} - model\|$, where $model$ is defined as: $C \cdot XES_{teo} + (1 - C)XES_{Ni(OH)_2}$, while C is the concentration of the theoretical spectrum present in the bi-component mixture. No further energy shift was applied to the theoretical spectra.

The result of this approach is reported in **Figure 9**, showing a good agreement between theoretical and experimnetal XES spectra. Iparticular, for the state during the CO$_2$RR conditions, the concentration of the Ni species bound to the two CO groups obtained by the XES fit is 0.32. This value is very close to the average concentration value of this species, as obtained from HERFD XANES analysis in **Figure 4**(b) (ca. 0.37).
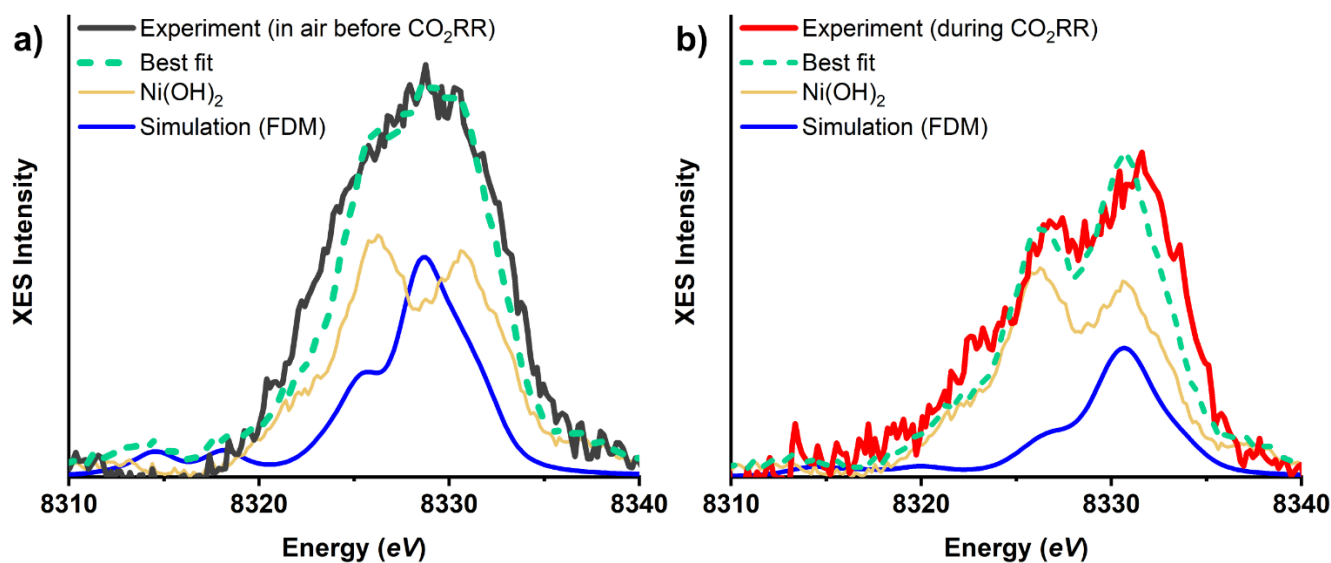

Figure 9: Comparison between the experimental and reconstructed (best fit) spectra: before the CO$_2$RR a) and during CO$_2$RR b). Partials contributions of each component are shown weighted by their related concentration value.

References:
1. Ju, W., et al., *Understanding activity and selectivity of metal-nitrogen-doped carbon catalysts for electrochemical reduction of CO2.* Nature Communications, 2017. **8**.

2. Timoshenko, J. and B.R. Cuenya, *In Situ/Operando Electrocatalyst Characterization by X-ray Absorption Spectroscopy.* Chemical Reviews, 2021. **121**(2): p. 882-961.

3. Li, C., et al., *Covalent Organic Framework (COF) Derived Ni-N-C Catalysts for Electrochemical CO2 Reduction: Unraveling Fundamental Kinetic and Structural Parameters of the Active Sites.* Angewandte Chemie International Edition, 2022. **61**(15): p. e202114707.

4. Manceau, A., M. Marcus, and T. Lenoir, *Estimating the number of pure chemical components in a mixture by X-ray absorption spectroscopy.* Journal of Synchrotron Radiation, 2014. **21**: p. 1140-1147.

5. Martini, A. and E. Borfecchia, *Spectral Decomposition of X-ray Absorption Spectroscopy Datasets: Methods and Applications.* Crystals, 2020. **10**(8).

6. Martini, A., et al., *PyFitit: The software for quantitative analysis of XANES spectra using machine-learning algorithms.* Computer Physics Communications, 2020. **250**: p. 15.

7. Jaumot, J., et al., *A graphical user-friendly interface for MCR-ALS: a new tool for multivariate curve resolution in MATLAB.* Chemometrics and Intelligent Laboratory Systems, 2005. **76**(1): p. 101-110.

8. Guda, A.A., et al., *Quantitative structural determination of active sites from in situ and operando XANES spectra: From standard ab initio simulations to chemometric and machine learning approaches.* Catalysis Today, 2019. **336**: p. 3-21.

9. Guda, S.A., et al., *Optimized Finite Difference Method for the Full-Potential XANES Simulations: Application to Molecular Adsorption Geometries in MOFs and Metal-Ligand Intersystem Crossing Transients.* Journal of Chemical Theory and Computation, 2015. **11**(9): p. 4512-4521.